ENTROPY GENERATION ANALYSIS OF THE REVISED CHENG-MINKOWYCZ PROBLEM FOR NATURAL CONVECTIVE BOUNDARY LAYER FLOW OF NANOFLUID IN A POROUS MEDIUM

by

Mohammad Mehdi RASHIDI[a,b]*, Amir Basiri PARSA[c], Leila SHAMEKHI[c], and Ebrahim MOMONIAT[d]

[a] Shanghai Key Laboratory of Vehicle Aerodynamics and Vehicle Thermal Management Systems, Jiading, Shanghai, China
[b] ENN-Tongji Clean Energy Institute of Advanced Studies, Shanghai, China
[c] Young Researchers and Elite Club, Hamedan Branch, Islamic Azad University, Hamedan, Iran
[d] Center for Differential Equations, Continuum Mechanics and Applications School of Computational and Applied Mathematics, University of the Witwatersrand, Johannesburg, South Africa

Original scientific paper
DOI: 10.2298/TSCI15S1S69R

The similar solution on the equations of the revised Cheng-Minkowycz problem for natural convective boundary layer flow of nanofluid through a porous medium gives (using an analytical method), a system of non-linear partial differential equations which are solved by optimal homotopy analysis method. Effects of various drastic parameters on the fluid and heat transfer characteristics have been analyzed. A very good agreement is observed between the obtained results and the numerical ones. The entropy generation has been derived and a comprehensive parametric analysis on that has been done. Each component of the entropy generation has been analyzed separately and the contribution of each one on the total value of entropy generation has been determined. It is found that the entropy generation as an important aspect of the industrial applications has been affected by various parameters which should be controlled to minimize the entropy generation.

Key words: *entropy generation, nanofluid, optimal homotropy analysis method, porous media*

Introduction

One of the most applicable methods for increasing the coefficient of heat transfer is suspending ultrafine solid particles in a convectional fluid. Many researchers have continued this presented field by Choi and Eastman [1] experimentally and numerically [2-5]. The Cheng-Minkowycz problem of natural convection past a vertical plate is studied analytically by Kuznetsov and Nield [6, 7]. In recent decades, many attempts have been done on the newly developed methods to introduce an analytic solution of non-linear equations; one of these is differential transform method that has been used in recent years frequently [8, 9]. In 1992, Liao [10] introduced the basic ideas of the homotopy in topology to propose a general analytic method for nonlinear problems, namely homotopy analysis method (HAM) that does not need

* Corresponding author; e-mail: mm_rashidi@tongji.edu.cn

to any small parameter. This method has been successfully applied to solve many types of non-linear problems by others [11, 12].

Since entropy generation analysis is used to optimize the thermal engineering devices for higher energy efficiency [13], it has been attracted a wide attention on its applications and rates in recent years. In order to access the best thermal design of systems, by minimizing the irreversibility, the second law of thermodynamics could be employed. Entropy generation is a criterion of the destruction of the available system work [14-17]. In this paper, at first an analytical study is done on the revised Cheng-Minkowycz problem for natural convective boundary layer flow in a porous medium saturated by a nanofluid using optimal homotropy analysis method (OHAM). Then a full formulation of entropy generation has been derived and analyzed parametrically as a new study.

Flow analysis and mathematical formulation

Let us consider the 2-D problem of revised Cheng-Minkowycz problem for natural convection past a vertical plate in a porous medium saturated by a nanofluid. First spatial coordinate, x, is aligned vertically upward just fitted on the vertical plate and the second one, y, is aligned horizontally such that the plate is at $y = 0$. In this problem for nanofluid Buongiorno's model has been utilized to incorporate the effects of Brownian motion and thermophoresis. The Oberbeck-Boussinesq approximation is employed. For the porous medium the Darcy model is employed and homogeneity and local thermal equilibrium is assumed.

The Navier-Stokes equations governing the motion of the mentioned problem take the form by scale analysis [7]:

$$\frac{\partial u}{\partial x}+\frac{\partial v}{\partial y}=0 \tag{1}$$

$$\frac{\partial P}{\partial x}=-\frac{\mu}{K}u+[(1-\phi_\infty)\rho_{f\infty}\beta(T-T_\infty)-(\rho_P-\rho_{f\infty})(\phi-\phi_\infty)]\mathrm{g}, \quad \frac{\partial P}{\partial y}=0 \tag{2}$$

$$u\frac{\partial T}{\partial x}+v\frac{\partial T}{\partial y}=\alpha_m\nabla^2 T+\tau\left[D_B\frac{\partial \phi}{\partial y}\frac{\partial T}{\partial y}+\frac{D_T}{T_\infty}\left(\frac{\partial T}{\partial y}\right)^2\right] \tag{3}$$

$$\frac{1}{\varepsilon}\left(u\frac{\partial \phi}{\partial x}+v\frac{\partial \phi}{\partial y}\right)=D_B\frac{\partial^2 \phi}{\partial y^2}+\left(\frac{D_T}{T_\infty}\right)\frac{\partial^2 T}{\partial y^2} \tag{4}$$

The boundary conditions are introduced as:

$$\begin{gathered} D_B\frac{\partial \phi}{\partial y}+\frac{D_B}{T_\infty}\frac{\partial T}{\partial y}=0, \quad v=0, \quad T=T_w, \quad \text{at } y=0 \\ u\to 0, \quad v\to 0, \quad T\to T_\infty, \quad \phi\to\phi_\infty, \quad \text{as } y\to\infty \end{gathered} \tag{5}$$

To obtain the system of non-dimensional ordinary differential equations form of the above equations, first the pressure P has been eliminated from eq. (2) by cross-differentiation, and the following similarity transforms variables have been introduced using the stream function ψ [7]:

$$\eta=\sqrt{\mathrm{Ra}_x}\frac{y}{x}, \quad s(\eta)=\frac{\psi}{\alpha_m\sqrt{\mathrm{Ra}_x}}, \quad \theta(\eta)=\frac{T-T_\infty}{T_w-T_\infty}, \quad f(\eta)=\frac{\phi-\phi_\infty}{\phi_\infty} \tag{6}$$

Replacing these transformations into eqs. (1) to (4) gives the non-linear ordinary differential equations:

$$s'' - \theta' + Nrf' = 0 \tag{7}$$

$$\theta'' + \frac{1}{2}s\theta' + Nb\, f'\theta' + Nt(\theta')^2 = 0 \tag{8}$$

$$f'' + \frac{1}{2}\mathrm{Le}\, f' + \frac{Nt}{Nb}\theta'' = 0 \tag{9}$$

The boundary conditions become:

$$\begin{aligned} &s(0) = 0, \quad \theta(0) = 1, \quad Nb\, f'(0) + Nt\,\theta'(0) = 0, \\ &s'(\eta) \to 0, \quad \theta(\eta) \to 0, \quad f(\eta) \to 0, \quad \text{as } \eta \to \infty \end{aligned} \tag{10}$$

Entropy generation

The second law of thermodynamics can be applied to the homogeneous porous medium to yield the volumetric entropy generation rate as [18]:

$$\dot{S}'''_{gen} = \frac{k_{nf}}{{T_\infty}^2}(\nabla T)^2 + \frac{\mu_{nf}}{KT_\infty}\vec{v}^2 + \frac{\mu_{nf}}{T_\infty}\Phi \tag{11}$$

where in a two dimensional Cartesian co-ordinates we have:

$$(\nabla T)^2 = \left[\left(\frac{\partial T}{\partial x}\right)^2 + \left(\frac{\partial T}{\partial y}\right)^2\right], \quad \Phi = 2\left[\left(\frac{\partial u}{\partial x}\right)^2 + \left(\frac{\partial v}{\partial y}\right)^2\right] + \left(\frac{\partial u}{\partial y} + \frac{\partial v}{\partial x}\right)^2, \quad \vec{v}^2 = u^2 + v^2 \tag{12}$$

The first term on the right-hand side of equation Φ represents the entropy generation due to the heat transfer irreversibility, the second term represents the viscous dissipation (irreversibility) term for porous media and it is important for the Darcy flow model and the third term is the extra viscous dissipation term for the non-Darcy flow model.

Therefore, the entropy generation rate of this triple diffusive free convection along a horizontal plate in porous media saturated by a Darcy model nanofluid and two different salts is obtained as:

$$\begin{aligned} \dot{S}'''_{gen} = {} & \frac{k_{nf}}{T_\infty^2}\left[\left(\frac{\partial T}{\partial x}\right)^2 + \left(\frac{\partial T}{\partial y}\right)^2\right] + \frac{\mu_{nf}}{KT_\infty}(u^2 + v^2) + \frac{RD}{\phi_\infty}\left[\left(\frac{\partial \phi}{\partial x}\right)^2 + \left(\frac{\partial \phi}{\partial y}\right)^2\right] + \\ & + \frac{RD}{T_\infty}\left[\left(\frac{\partial T}{\partial x}\right)\left(\frac{\partial \phi}{\partial x}\right) + \left(\frac{\partial T}{\partial y}\right)\left(\frac{\partial \phi}{\partial y}\right)\right] \end{aligned} \tag{13}$$

The velocity components could be obtained from stream function in eq. (6):

$$u = \frac{\partial \psi}{\partial y} = \frac{\alpha_m}{x}\mathrm{Ra}_x s'(\eta), \quad v = -\frac{\partial \psi}{\partial x} = -\frac{\alpha_m}{2x}\sqrt{\mathrm{Ra}_x}\, s(\eta) + \frac{\alpha_m}{2x}\sqrt{\mathrm{Ra}_x}\,\eta s'(\eta) \tag{14}$$

The mentioned derivations also have been obtained from eq. (6) as:

$$\frac{\partial T}{\partial y} = \frac{\Delta T}{x}\sqrt{\mathrm{Ra}_x}\,\theta'(\eta), \quad \frac{\partial T}{\partial x} = -\frac{\Delta T}{2x}\eta\theta'(\eta), \quad \frac{\partial \phi}{\partial y} = \frac{\phi_\infty}{x}\sqrt{\mathrm{Ra}_x}\, f'(\eta), \quad \frac{\partial \phi}{\partial x} = -\frac{\phi_\infty}{2x}\eta f'(\eta) \tag{15}$$

Equation (13) can be simplified:

$$N_G = K_\mu \left\{ \frac{\mathrm{Ra}_x}{4x^2}[s(\eta)]^2 - \frac{\mathrm{Ra}_x}{2x^2}[\eta s(\eta)s'(\eta)] + \frac{\mathrm{Ra}_x^2}{x^2}[s'(\eta)]^2 + \frac{\mathrm{Ra}_x}{4x^2}[\eta s'(\eta)]^2 \right\} +$$
$$+K_C \left\{ \frac{\mathrm{Ra}_x}{x^2}[f'(\eta)]^2 + \frac{1}{4x^2}[\eta f'(\eta)]^2 - \frac{\mathrm{Ra}_x}{x^2}[f'(\eta)\theta'(\eta)] - \frac{1}{4x^2}\eta^2[f'(\eta)\theta'(\eta)] \right\} +$$
$$+K_{TC} \left\{ \frac{\mathrm{Ra}_x}{x^2}[f'(\eta)\theta'(\eta)] + \frac{1}{4x^2}\eta^2[f'(\eta)\theta'(\eta)] \right\} + K_{TH} \left\{ \frac{\mathrm{Ra}_x}{x^2}[\theta'(\eta)]^2 + \frac{1}{4x^2}[\eta\theta'(\eta)]^2 \right\} \tag{16}$$

OHAM solutions

The basic ideas of OHAM are documented in [10]. From eqs. (7)-(9) with boundary conditions (10), the initial approximations of $S(\eta), \Theta(\eta)$, and $F(y)$ are chosen as $S_0(y) = \mathrm{e}^{-\eta}$, $\Theta_0(\eta) = 1 - \mathrm{e}^{-\eta}$, $\mathrm{F}_0(\eta) = (Nt/Nb)\mathrm{e}^{-\eta}$. Selection criteria of initial approximations is satisfaction of boundary conditions, thus they are not unique. The linear operators are defined as:

$$\mathcal{L}[S(\eta;p)] = \frac{\partial^2 S(\eta;p)}{\partial\eta^2},\ \mathcal{L}[\Theta(\eta;p)] = \frac{\partial^2 \Theta(\eta;p)}{\partial\eta^2},\ \mathcal{L}[F(\eta;p)] = \frac{\partial^2 F(\eta;p)}{\partial\eta^2} - \frac{\partial F(\eta;p)}{\partial\eta} \tag{17}$$

Furthermore, eqs. (7)-(9) suggest the definitions of the non-linear operators:

$$\mathcal{N}[S(\eta;p)] = \frac{\partial^2 S(\eta;p)}{\partial\eta^2} - \frac{\partial\Theta(\eta;p)}{\partial\eta} + Nr\frac{\partial F(\eta;p)}{\partial\eta} \tag{18}$$

$$\mathcal{N}[\Theta(\eta;p)] = \frac{\partial^2\Theta(\eta;p)}{\partial\eta} + \frac{1}{2}S(\eta;p)\frac{\partial\Theta(\eta;p)}{\partial\eta} + Nb\frac{\partial F(\eta;p)}{\partial\eta}\frac{\partial\Theta(\eta;p)}{\partial\eta} +$$
$$+Nt\frac{\partial\Theta(\eta;p)}{\partial\eta}\frac{\partial\Theta(\eta;p)}{\partial\eta} \tag{19}$$

$$\mathcal{N}[F(\eta;p)] = \frac{\partial^2 F(\eta;p)}{\partial\eta^2} + \frac{1}{2}\mathrm{Le}\,S(\eta;p)\frac{\partial F(\eta;p)}{\partial\eta} + \frac{Nt}{Nb}\frac{\partial^2\Theta(\eta;p)}{\partial\eta^2} \tag{20}$$

Using the definition, with assumption auxiliary functions [10] $H_S(\eta) = 1$, $H_\Theta(\eta) = 1$, $H_F(\eta) = 1$, the zero-order deformation equation has been constructed as:

$$(1-p)\mathcal{L}[\varphi(x;p) - u_0(x)] = H_\varphi(x)p\hbar\mathcal{N}[\varphi(x;p)] \tag{21}$$

subject to the initial conditions:

$$\begin{aligned} &S_m = 0, \quad \Theta_m = 0, \quad Nb\,F'_m + Nt\,\Theta'_m = 0 \quad \text{at:}\ \ \eta = 0, \\ &S'_m \to 0, \quad \Theta_m \to 0, \quad F_m \to 0 \quad \text{as:}\ \ \eta \to \infty \end{aligned} \tag{22}$$

where

$$R_m(\vec{\mathrm{S}}_{m-1}) = \frac{\partial^2 S_{m-1}(\eta)}{\partial\eta^2} - \frac{\partial\Theta_{m-1}(\eta)}{\partial\eta} + Nr\frac{\partial F_{m-1}(\eta)}{\partial\eta} \tag{23}$$

$$R_m(\vec{\Theta}_{m-1}) = \frac{\partial^2 \Theta_{m-1}(\eta)}{\partial \eta^2} + \frac{1}{2}\sum_{j=0}^{m-1} S_j(\eta)\frac{\partial \Theta_{m-1-j}(\eta)}{\partial \eta} + Nb\sum_{j=0}^{m-1}\frac{\partial F_j(\eta)}{\partial \eta}\frac{\partial \Theta_{m-1-j}(\eta)}{\partial \eta} + \\ + Nt\sum_{j=0}^{m-1}\frac{\partial \Theta_j(\eta)}{\partial \eta}\frac{\partial \Theta_{m-1-j}(\eta)}{\partial \eta} \tag{24}$$

$$R_m(\vec{\mathrm{F}}_{m-1}) = \frac{\partial^2 F_{m-1}(\eta)}{\partial \eta^2} + \frac{1}{2}\mathrm{Le}\sum_{j=0}^{m-1} S_j(\eta)\frac{\partial F_{m-1-j}(\eta)}{\partial \eta} + \frac{Nt}{Nb}\frac{\partial^2 \Theta_{m-1}(\eta)}{\partial \eta^2} \tag{25}$$

The solution of the m^{th} order deformation for $m \geq 1$ can be done simply. The final approximate solution can be obtained:

$$S_{a\,pp} = \sum_{i=0}^{n} S_i, \quad \Theta_{a\,pp} = \sum_{i=0}^{n}\Theta_i, \quad F_{a\,pp} = \sum_{i=0}^{n} F_i$$

In general, by means of the so-called $\hbar$-curve by Liao [10], the valid region of $\hbar$ is the horizontal line segment. To see the range of admissible values of the auxiliary parameter $\hbar$ the curves of $\hbar$ are plotted in fig. 1 associated with the 20[th] order approximation. The optimal value of auxiliary parameter is obtained as:

$$E_{S,m} = \frac{1}{K}\sum_{i=0}^{K}\left[\mathcal{N}_S \sum_{i=0}^{m} S_i(i\Delta x)\right]^2, \quad E_{\Theta,m} = \frac{1}{K}\sum_{i=0}^{K}\left[\mathcal{N}_\Theta \sum_{i=0}^{m} \Theta_i(i\Delta x)\right]^2, \\ E_{F,m} = \frac{1}{K}\sum_{i=0}^{K}\left[\mathcal{N}_F \sum_{i=0}^{m} F_i(i\Delta x)\right]^2 \tag{26}$$

where $\Delta x = 10/K$ and $K = 20$. For a given order of approximation, m, the optimal values $\hbar$ are given by the minimum of E_m, corresponding to the nonlinear algebraic equations:

$$\frac{\mathrm{d}E_{F,m}}{\mathrm{d}\hbar} = 0, \qquad \frac{\mathrm{d}E_{\Theta,m}}{\mathrm{d}\hbar} = 0, \qquad \frac{\mathrm{d}E_{F,m}}{\mathrm{d}\hbar} = 0 \tag{27}$$

Table 1 shows the optimal values obtained for the auxiliary parameter $\hbar$. To see the accuracy of the solutions, the residual errors are calculated for the system.

Figures 2-4 show the residual errors given by 20[th] order approximation.

In these figures the best selection of $\hbar$ for the best accuracy can be found.

Table 1. The optimal values of $\hbar$ for different values of Le, *Nb, Nr,* and *Nt*

Series solution	Le	1.0	10.0	100.0
	Nb	0.5	0.3	0.1
	Nr	0.5	0.1	0.3
	Nt	0.5	0.3	0.1
$s'(y)$		$\hbar_{\text{optimal}} = -0.7567$	$\hbar_{\text{optimal}} = -0.7163$	$\hbar_{\text{optimal}} = -0.5434$
$\theta(\eta)$		$\hbar_{\text{optimal}} = -0.8342$	$\hbar_{\text{optimal}} = -0.4594$	$\hbar_{\text{optimal}} = -0.1884$
$f(\eta)$		$\hbar_{\text{optimal}} = -0.7023$	$\hbar_{\text{optimal}} = -0.6788$	$\hbar_{\text{optimal}} = -0.4355$

Figure 5 shows $s(\eta)$, $s'(\eta)$, $\theta(\eta)$, and $f(\eta)$ obtained by the OHAM and numerical method (fourth-order Runge-Kutta quadrate with a shooting method).

Table 2. Comparison of values of $s'(\eta)$ obtained by various orders of the OHAM with numerical solution

η	$s'(\eta)$ (Le = 1.0, Nr = 0.5, Nb = 0.5, Nt = 0.5)		
	OHAM order 10	OHAM order 20	Numerical
0	1.445577	1.151949	1.152334
2	0.344455	0.234595	0.234667
4	0.122333	0.012916	0.013653
6	–0.034444	–0.00816	0.005777

A good agreement between analytical and numerical methods can be found.

For example, tab. 2 shows the comparison of values of s′(η), obtained by various orders of the OHAM with numerical solution.

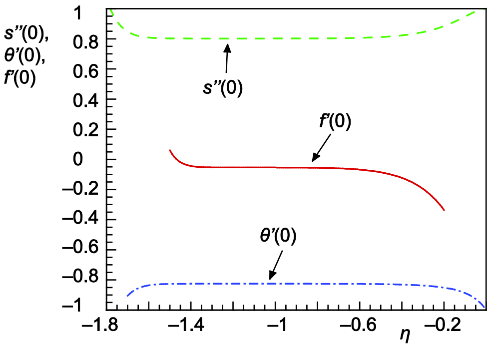

Figure 1. The $\hbar$-curves given by the 20th order approximate solution

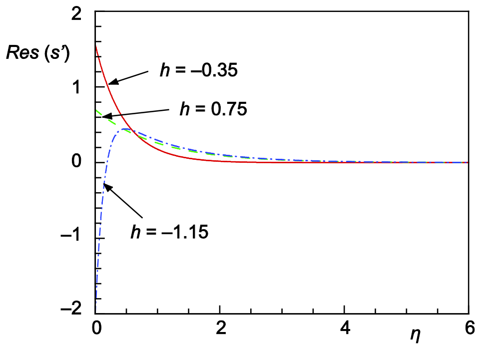

Figure 2. The behavior of the solutions obtained by the OHAM for various $\hbar$

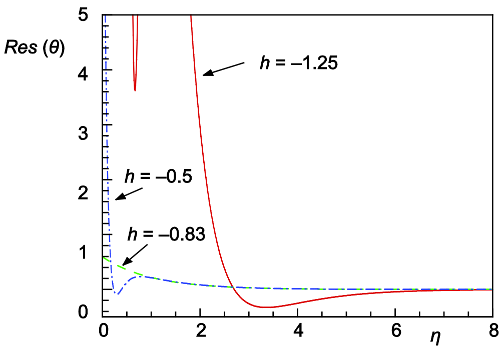

Figure 3. The behavior of the solutions obtained by the OHAM for various $\hbar$

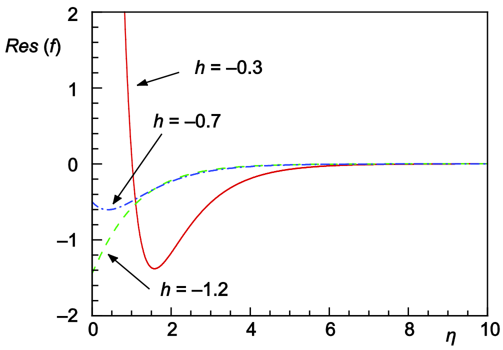

Figure 4. The behavior of the solutions obtained by the OHAM for various $\hbar$

Results and discussions

The OHAM has been applied successfully to derive the semi-numerical solutions under appropriate boundary conditions on the governing 2-D partial differential equations.

As can be seen in fig. 5 a good agreement between results of analytical and numerical solutions can be found. Figure 6 shows variation of $f(\eta)$ with respect to η for different values of Lewis number.

Analyses of Brownian motion parameter have been presented in fig. 7. The longitudinal component of the velocity increases in boundary layer with increasing Nb. Effect of thermophoresis parameter has been discussed by fig. 8. According to this figure it is interesting that as η increases the value of $f(\eta)$ rises to a maximum before decaying to zero. The most important aspect of study is entropy generation analysis. As a good result in figs. 9 to 15, it is noticeable that the effective parameters could be classified into two classes. The class 1 contains the parameters which by increasing them, the entropy generation increases and the class 2 contains the others that by increasing in them the entropy generation decreases. The importance of this classification is its use for minimizing entropy generation in the industrial applications. Class 1 contains Nr, Ra, K_μ, K_C, and K_{TH}. Class 2 contains Nb, Nt, and Le.

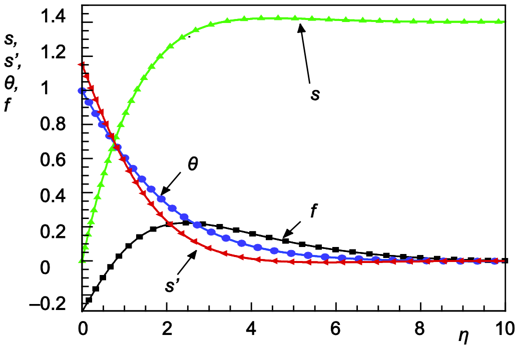

Figure 5. Comparison of obtained results by the 20th order approximation OHAM

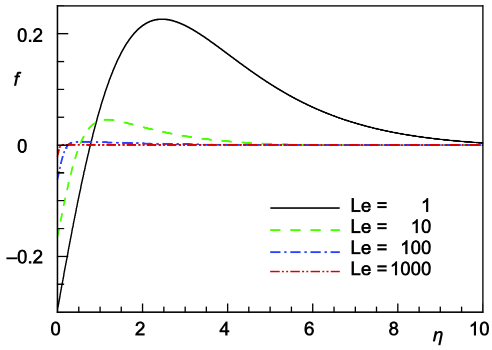

Figure 6. Variation of $f(\eta)$ for Lewis number

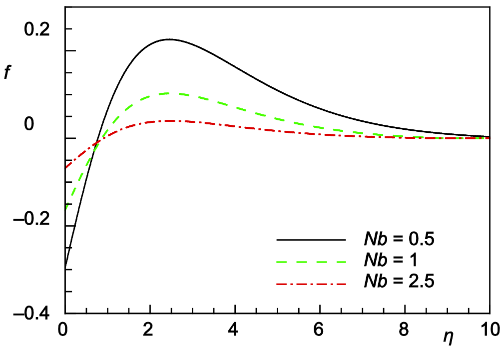

Figure 7. Variation of $f(\eta)$ for Brownian motion parameter

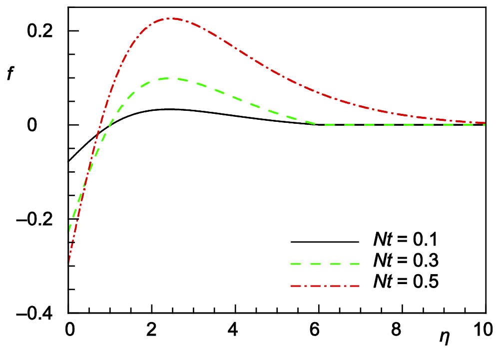

Figure 8. Variation of $f(\eta)$ for thermophoresis parameter

As can be seen in fig. 16, the contribution of entropy generation value caused by K_{TC} in the total value of entropy generation is not considerable, so the effect of this parameter has not been analyzed. The manners of changes, ranges of these changes and all other important keys are shown in these figures and are very useful for design of different applications. In all of these figures constant parameters, except those highlighted in each figure, have the values as tabulated in tab. 3. In fig. 9 effect of Nt on the entropy generation has been illustrated. It is clear that Nt has an ambivalent effect on N_G.

Table 3. Constant values of physical parameters

Nt	Nb	Nr	Le	Ra_x	K_μ	K_C	K_{TC}	K_{TH}	x
0.5	0.5	0.5	10	100	0.001	0.05	0.01	0.8	0.2

It means that increasing in Nt causes N_G to decrease at first up to a certain point about 1, then it makes opposite effect, so this can be a key point in designing of the industrial applications. Based on the presented curves in figs. 10 and 11, Nb and Le have the same effect on N_G, with increasing in them, N_G has a limit decreasing. In contrast with these parameters, as can be seen in fig. 12, Ra has a concurrent and considerable effect on N_G. Concurrent means the increase in N_G for increasing in Ra.

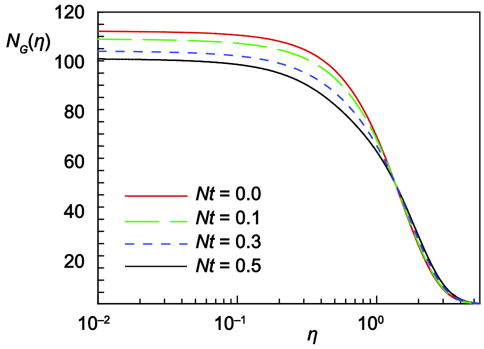

Figure 9. Variation of entropy generation for thermophoresis parameter

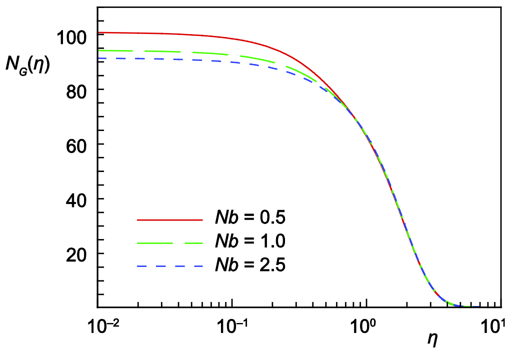

Figure 10. Variation of entropy generation for Brownian motion parameter

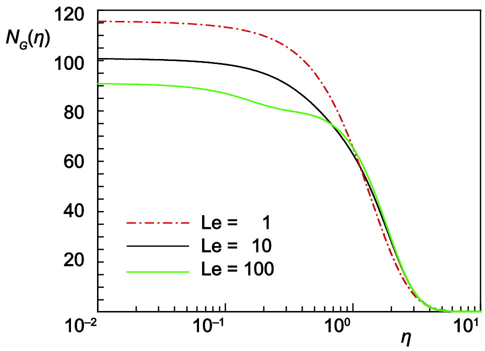

Figure 11. Variation of entropy generation for different values of Lewis number

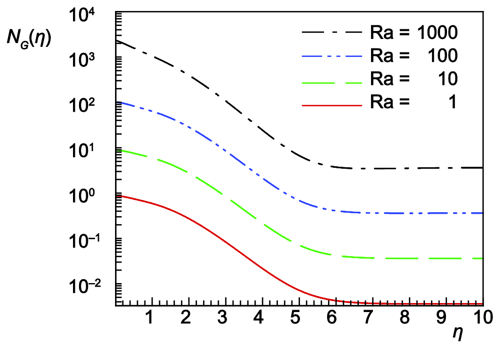

Figure 12. Variation of entropy generation for Rayleigh number

Figures 13 to 15 show the effect of different irreversibility distribution ratios on N_G. It is clear that increasing in irreversibility distribution ratios causes increasing in the value of N_G. It can be mentioned that K_μ has the highest effect on N_G. Also the effect of K_{TH} is higher than the effect of K_C on N_G. With this knowledge, now the industrial design from the point of view of N_G is quite perfect and scientific. The share of each term in the total value of entropy generation has been shown in fig. 16.

Conclusions

In this paper the revised Cheng-Minkowycz problem for natural convective boundary layer flow of nanofluid through a porous medium has been solved analytically by using optimal homotopy analysis method. A parametric analysis on the problem is presented. Then as the main goal of this study, a comprehensive parametric analysis on the dimensionless entropy generation was done and effects of the physical parameters on the problem were shown. Each component of the entropy generation has been analyzed separately, and the share of each one on the total value of entropy generation has been determined. The results contain very important subjects which have great roles in designing the industrial applications.

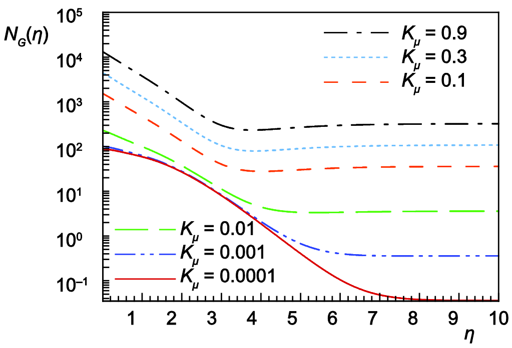

Figure 13. Variation of entropy generation for coefficient due to viscous irreversibility

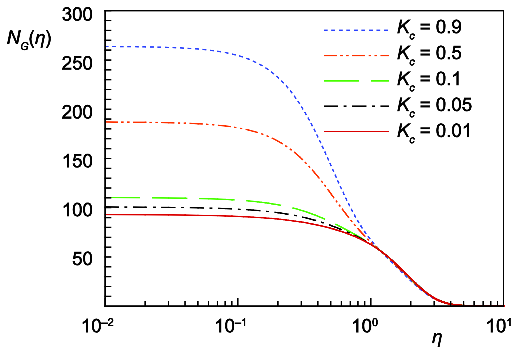

Figure 14. Variation of entropy generation for coefficient due to nanoparticle volume fraction

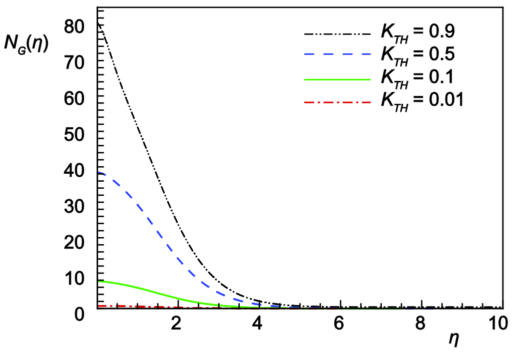

Figure 15. Variation of entropy generation for coefficient due to heat transfer irreversibility

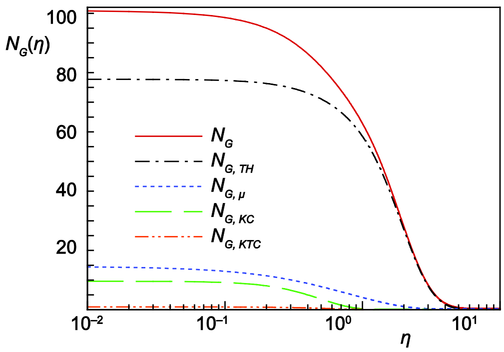

Figure 16. Comparison of entropy generation terms

Nomenclature

D – mass diffusivity, [m^{2}s^{-1}]
D_B – Brownian diffusion coefficient, [m^{2}s^{-1}]
D_T – thermophoretic diffusion coefficient, [m^{2}s^{-1}]
f – rescaled nanoparticle volume fraction, defined by eq. (6)
g – acceleration due to gravity, [ms^{-2}]
k_m – effective thermal conductivity of the porous medium, [Wm^{-1}K^{-1}]
K – permeability of the porous medium
K_c – entropy generation coefficient due to nanoparticle volume fraction [$=RDC_\infty/k_{nf}\,(T_\infty/\Delta T)^2$], [–]
K_{TC} – entropy generation coefficient due to mixed product of concentration and thermal effect of nanofluid [$=RDT_\infty/k_{nf}\,(C_\infty/\Delta T)$], [–]
K_{Th} – entropy generation coefficient due to heat transfer irreversibility [$=(T_\infty/\Delta T-1)^2$], [–]
K_μ – entropy generation coefficient due to viscous irreversibility [$=(\mu T_\infty)/(k_{nf}K)\,(\alpha_m/\Delta T)^2$], [–]
$\mathcal{L}$ – linear operator of the OHAM
Le – Lewis number [$=\alpha_m/(\varepsilon D_B)$], [–]
$\mathcal{N}$ – nonlinear operator of the OHAM
N_G – entropy generation rate
Nb – Brownian motion parameter [$=(\tau D_B\phi_\infty)/\alpha_m$], [–]
Nr – nanofluid buoyancy ratio {$=[(\rho_p-\rho_{f\infty})\phi_\infty]/[\rho_{f\infty}\beta_T(T_w-T_\infty)(1-\phi_\infty)]$}, [–]
Nt – thermophoresis parameter {$=[\tau D_T(T_w-T_\infty)]/T_\infty\alpha_m$}, [–]
Ra$_x$ – local Rayleigh number {$=[(1-\phi_\infty)\,\rho_{f\infty}gK\beta_T x]/\mu\alpha_m$}, [–]
s – dimensionless stream function, defined by eq. (6)
ΔT – temperature difference ($=T_w-T_\infty$), [K]

Greek symbols

α_m – thermal diffusivity of porous medium [$= k_m/(\rho c_p)_f$], [–]
β – volumetric thermal expansion coefficient of the fluid
η – similarity variable, defined by eq. (6)
θ – dimensionless temperature, defined by eq. (6)
μ – absolute viscosity of the base fluid, [$\text{kgs}^{-1}\text{m}^{-1}$]
ν – kinematic viscosity of the fluid, [m^2s^{-1}],
ϕ – nanoparticle volume fraction, [–]
ϕ_∞ – ambient nanoparticle volume fraction, [–]

Subscripts

f – fluid phase
m – porous medium
nf – nanofluid
w – condition of the wall
∞ – condition of the free steam

References

[1] Choi, S. U. S., Eastman, J. A., Enhancing Thermal Conductivity of Fluids with Nanoparticles, *Materials Science, 231* (1995), 8, pp. 99-105
[2] Rashidi, M. M., Erfani, E., The Modified Differential Transform Method for Investigating Nano Boundary-Layers over Stretching Surfaces, *International Journal of Numerical Methods for Heat & Fluid Flow, 21* (2011), 7, pp. 864-883
[3] Rashidi, M. M., *et al.*, DTM-Pade Modeling of Natural Convective Boundary Layer Flow of a Nanofluid past a Vertical Surface, *Int. Journal of Thermal and Environmental Engineering, 4* (2011), 1, pp. 13-24
[4] Khan, Z. H., *et al.*, Triple Diffusive Free Convection along a Horizontal Plate in Porous Media Saturated by a Nanofluid with Convective Boundary Condition, *International Journal of Heat and Mass Transfer, 66* (2013), 1, pp. 603-612
[5] Buongiorno, J., Convective Transport in Nanofluids, *ASME J. Heat Transfer, 128* (2006), 1, pp. 240-250
[6] Kim, S., Vafai, K., Analysis of Natural-Convection about a Vertical Plate Embedded in a Porous-Medium, *Int. J. Heat Mass Transfer, 32* (1989), 4, pp. 665-677
[7] Kuznetsov, A. V., Nield, D. A., The Cheng-Minkowycz Problem for Natural Convective Boundary Layer Flow in a Porous Medium Saturated by a Nanofluid: A Revised Model, *International Journal of Heat and Mass Transfer, 65* (2013), 1, pp. 682-685
[8] Erfani, E., *et al.*, The Modified Differential Transform Method for Solving off-Centered Stagnation Flow towards a Rotating Disc, *International Journal of Computational Methods, 7* (2010), 4, pp. 655-670
[9] Rashidi, M. M., *et al.*, Analytical Modeling of Heat Convection in Magnetized Micropolar Fluid by Using Modified Differential Transform Method, *Heat Transfer-Asian Research, 40* (2011), 3, pp. 187-204
[10] Liao, S. J., The Proposed Homotopy Analysis Technique for the Solution of Nonlinear Problems, Ph. D. thesis, Shanghai Jiao Tong University, Shanghai, China, 1992
[11] Rashidia, M. M.,*et al.*, Analytic Approximate Solutions for Steady Flow over a Rotating Disk in Porous Medium with Heat Transfer by Homotopy Analysis Method, *Computers & Fluids, 54* (2012), 1, pp. 1-9
[12] Basiri Parsaa, A., *et al.*, Semi-Computational Simulation of Magneto-Hemodynamic Flow in a Semi-Porous Channel Using Optimal Homotopy and Differential Transform Methods, *Computers in Biology and Medicine, 43* (2013), 9, pp. 1142-1153
[13] Bejan, A., *Advances in Heat Transfer* (Eds. James, P. H., Thomas, F.I.), Elsevier, 1982
[14] Butt, A. S., *et al.*, Entropy Generation in the Blasius Flow under Thermal Radiation, *Physica Scripta, 85* (2012), 3, pp. 35-48
[15] Rashidi, M. M., *et al.,* Entropy Generation in Steady MHD Flow due to a Rotating Porous Disk in a Nanofluid, *International Journal of Heat and Mass Transfer, 62* (2013), 1, pp. 515-525
[16] Rashidi, M. M., *et al.,* Parametric Analysis of Entropy Generation in Off-Centered Stagnation Flow Towards a Rotating Disc, *Nonlinear Engineering, 3* (2014), 1, pp. 27-41
[17] Rashidi, M. M., *et al.,* Parametric Analysis of Entropy Generation in Magneto-Hemodynamic Flow in a Semi-Porous Channel with OHAM and DTM, *Applied Bionics and Biomechanics, 11* (2014), 1-2, pp. 47-60
[18] Baytas, A. C., Baytas, A. F., Entropy Generation in Porous Media, in: *Transport Phenomena in Porous Media III* (Eds. D. B. Ingham, I. Pop), Elsevier, Oxford. UK, 2005, pp. 201-224

Paper submitted: October 10, 2014
Paper revised: January 21, 2015
Paper accepted: February 2, 2015